Quantitative Susceptibility Mapping using Segmentation-Enabled Dipole Inversion

Jakob Meineke[1], Julien Senegas[1], Ulrich Katscher[1], and Fabian Wenzel[1]
[1]*Philips Research Europe, Hamburg, Hamburg, Germany*

Target Audience: Researchers interested in quantitative susceptibility mapping (QSM), neuro-degenerative diseases and iron-quantification.

Purpose: This work describes a method for QSM reconstruction which uses a priori knowledge from automated anatomical segmentation within a single step formulation of the inverse field-to-source problem. The proposed method is dubbed segmentation-enabled dipole inversion (SEDI) and applied to in vivo brain data of healthy volunteers and a numerical phantom for validation.

Theory: Starting from the measured off-resonance field map f, the susceptibility χ is computed by solving the following least-squares minimization problem, similar to [1]:

$$\chi = \arg\min \left\| W_1 \left(L\left(\frac{B_0\gamma}{2\pi} D(\chi)\right) - L(f) \right) \right\|_2^2 + \lambda \left\| W_2 \, \vec{G}(\chi) \right\|_2^2 , \qquad (1)$$

with B_0: external magnetic field, γ: gyromagnetic ratio, D: dipole operator, L: Laplacian, λ: regularization parameter, $\vec{G}$: gradient operator, W_1: binary mask for data-fidelity, W_2: binary mask for regularization. Applying the Laplacian L to the measured field f as well as $D(\chi)$ avoids separate removal of the background-field from f and integrates dipole inversion and background-field removal in a single step. W_2 is derived from W_1 by setting all voxels to zero, which were classified as belonging to a tissue boundary (edge). Here, to overcome the shortcomings of gradient-based edge detection, an edge mask is generated from region labels of an automated anatomical segmentation of a T1-weighted TFE scan. This edge-mask is combined with another mask obtained from thresholding the gradient of the magnitude image as in MEDI [2]. In this way, continuous edges are obtained and the decoupling of the susceptibilities in adjacent tissue segments is improved.

Methods: Susceptibility maps were computed for a numerical phantom and healthy volunteers (N=5) solving Eq. (1) using a preconditioned conjugate gradient approach [3]. For comparison, susceptibility maps were also computed using Eq. 1 but without edges from segmentation and using MEDI [2] after background-field removal with PDF [4] or SHARP [5]. Volunteers were scanned on a 3T scanner with an 15-channel head coil (Ingenia, Philips Healthcare, Best, The Netherlands) using a multi-echo gradient-echo sequence for QSM (FOV: (AP, FH, RL) 240×145×210 mm^3, acq voxel: 0.6×0.6×2.0 mm^3, FA=14°, TE=3.5 ms, ΔTE=4 ms, 7 echoes, TR=31 ms, bipolar readout, BW=275.9 Hz/vx, SENSE (P/S) 1.8x1.2) and a T1-weighted magnetization-prepared TFE sequence for model-based segmentation (FOV: (AP, FH, RL) 240×240×170 mm^3, acq voxel 0.94×0.94×1.0 mm^3, FA=8°, TR=8 ms, TFE factor=222, inversion delay 1000 ms, BW=191.5 Hz/vx, SENSE (P/S) 1.0/2.2). The T1-weighted scans were registered rigidly to the magnitude of the first echo of the QSM scans. Boundaries of 20 sub-cortical regions and the two hemispheres were segmented automatically by applying a shape-constrained deformable surface model [6] to the T1-weighted scans so that anatomical regions were available in the QSM scans. To quantitatively assess the performance of SEDI compared to the other methods, a numerical phantom was generated using the subcortical segmentation for volunteer 1 and the last echo magnitude of the corresponding QSM scan. Field maps were calculated including background from the water/air interfaces and Gaussian white noise.

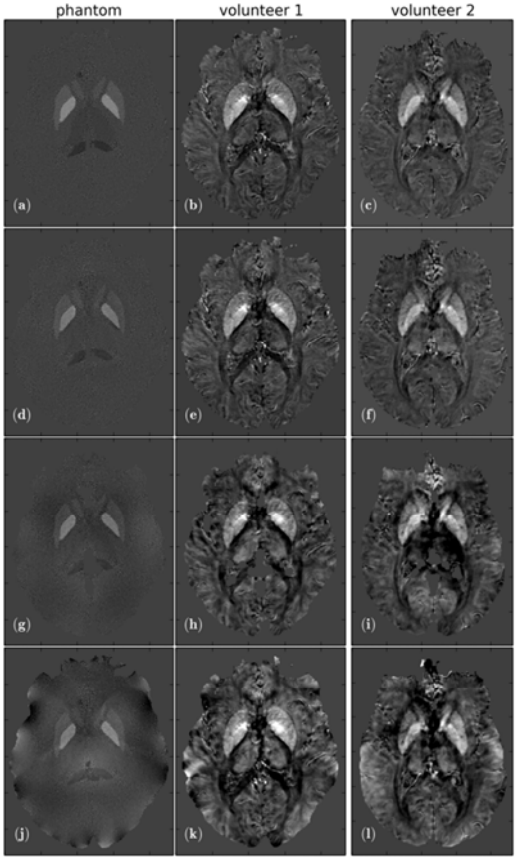

Figure 1: Susceptibility maps for phantom and volunteer data. (a)-(c): SEDI, i.e. Eq. (1) with edges from segmentation, (d)-(f): using Eq. (1) w/o edges from segmentation, (g)-(i): MEDI with SHARP, (j)-(l): MEDI with PDF. Grayscale for all images: -0.1 ppm (black) to 0.3 ppm (white).

Results: Table 1 summarizes the results of linear regression between reconstructed and input susceptibility for the numerical phantom. The slope reflects the accuracy of the reconstruction and is ideally equal to one. The columns of Figure 1 show susceptibility maps for the phantom data and for in vivo data from two selected volunteers, while the rows show the different reconstruction methods, see caption. For the phantom and the in vivo data, SEDI (row 1) shows more homogeneous susceptibility maps than either SHARP+MEDI or PDF+MEDI (rows 3 and 4). Without using edges from segmentation (row 2), the numerical phantom shows a bias in the reconstructed susceptibility, without affecting the homogeneity. For the numerical phantom and volunteer 1, the artifacts show a qualitatively similar behavior.

Method	slope	R^2
SEDI	0.990(4)	0.9996
Eq. (1) w/o segmentation	0.72(2)	0.97
SHARP + MEDI (with seg)	0.82(5)	0.93
PDF + MEDI (with seg)	0.84(7)	0.85

Table 1: Results of linear regression for the numerical phantom. Figures in parentheses are std of regression result.

Discussion and Conclusions: SEDI achieves the most accurate susceptibility reconstruction of the methods considered here for the numerical phantom. The reliable edge information from segmentation is a crucial input factor enabling the use of Eq. (1) for single-step dipole inversion and background-field removal. In vivo QSM with SEDI shows excellent susceptibility contrast with no visible artifacts from background-field removal, removing an important source of systematic error in measuring susceptibility in a given ROI, e.g. for iron-quantification.

Acknowledgements: This project has received funding from European Union's Seventh Framework Programme, grant no. 601055

References:[1] Sharma et al., MRM, 10.1002/mrm.25448; [2] de Rochefort et al., MRM 63, 194; [3] Bilgic et al., ISMRM2014, #0601; [4] Liu et al., NMR Biomed. 24, 1129; [5] Schweser et al., NeuroImage 54, 2789; [6] Ecabert et al., IEEE Transactions on Medical Imaging 27, 1189